NASA TECHNICAL NOTE

NASA TN D-5412

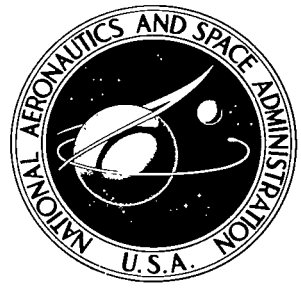

NASA TN D-5412

NATURAL FREQUENCY OF LIQUIDS IN ANNULAR CYLINDERS UNDER LOW GRAVITATIONAL CONDITIONS

by Thomas L. Labus

Lewis Research Center
Cleveland, Ohio

NATIONAL AERONAUTICS AND SPACE ADMINISTRATION • WASHINGTON, D. C. • SEPTEMBER 1969

NATURAL FREQUENCY OF LIQUIDS IN ANNULAR CYLINDERS UNDER LOW GRAVITATIONAL CONDITIONS

By Thomas L. Labus

Lewis Research Center
Cleveland, Ohio

NATIONAL AERONAUTICS AND SPACE ADMINISTRATION

For sale by the Clearinghouse for Federal Scientific and Technical Information
Springfield, Virginia 22151 – CFSTI price $3.00

ABSTRACT

As a part of the general study of liquid behavior in a low gravity environment, an experimental investigation was conducted to determine the natural frequency of liquid sloshing in annular cylinders. Static contact angles were restricted to near zero degrees. The experiments were conducted over a range of gravitational conditions, including normal gravity, such that the Bond numbers ranged from essentially 0 to approximately 200. The natural frequency for deep liquid depths was empirically correlated with known system parameters as a function of the Bond number.

NATURAL FREQUENCY OF LIQUIDS IN ANNULAR CYLINDERS UNDER LOW GRAVITATIONAL CONDITIONS

by Thomas L. Labus

Lewis Research Center

SUMMARY

As a part of the general study of liquid behavior in a low gravity environment, an experimental investigation was conducted to determine the natural frequency of liquid sloshing in annular cylinders. Static contact angles were restricted to near zero degrees. The experiments were conducted over a range of gravitational conditions, including normal gravity, such that the Bond numbers ranged from essentially 0 to approximately 200. The natural frequency for deep liquid depths was empirically correlated with known system parameters as a function of the Bond number.

INTRODUCTION

A knowledge of the characteristics of liquids in space vehicle tanks is important to design engineers. One important characteristic is that of liquid sloshing, which results in a changing center of mass and can affect vehicle stability and control. The characteristics of liquid sloshing have, therefore, been the subject of a considerable amount of study in recent years.

A summary of high Bond number liquid sloshing investigations and some of the original work in low Bond number asymmetric sloshing is contained in reference 1. (The Bond number is a measure of the relative importance of gravitational to capillary forces.) The natural frequency of liquids in cylinders was determined experimentally and correlated with the Bond number in references 2 and 3. These studies, however, were for the cylindrical geometry, which has received considerable attention because of its extensive use as a rocket vehicle propellant tank. The addition of internal instrumentation devices, or the compartmentization of cylindrical tanks, as cited in reference 1, causes a departure from the cylindrical geometry and can affect the natural frequency of the liquid. One of the geometric configurations that may result from internal

instrumentation and compartmentization is the annular cylinder. The annular geometry consists of a cylindrical rod located concentrically within a hollow cylindrical container. Previous investigations on the effect of the internal cylinder on the natural frequency (refs. 1, 4, and 5) have excluded the effects of surface tension. No information is available yielding the natural frequency in low Bond number environments, where surface tension forces are significant.

This report presents the experimental results of tests which examined the natural frequency in annular cylinders under Bond numbers ranging from essentially zero to approximately 200. The tests were conducted at NASA Lewis Research Center in both the 2.2- and 5-second zero gravity facilities. The natural frequency in annular cylinders was empirically correlated with known system parameters as a function of the Bond number. The liquids used exhibited contact angles very near zero degrees on the container walls. This study has been restricted to liquid depths greater than 2 outer cylinder radii.

SYMBOLS

a	system acceleration, cm/sec^2
Bo	Bond number ($Bo = aR^2/\beta$)
f_1	theoretical constant
f_2	empirical constant
g_0	acceleration due to gravity, 980 cm/sec^2
h	lowest point on interface measured from cylinder bottom, cm
R	outer cylinder radius, cm
r	inner cylinder radius, cm
r/R	annulus ratio
t	time, sec
X_l	instantaneous displacement of edge, cm
β	specific surface tension ($\beta = \sigma/\rho$), cm^3/sec^2
θ	contact angle, deg
ρ	liquid density, g/cm^3
σ	surface tension, dynes/cm; N/cm
Ω_c^2	cylindrical natural frequency parameter, $\Omega_c^2 = (\omega_c)^2 R^3/\beta$

Ω_A^2 annular natural frequency parameter, $\Omega_A^2 = (\omega_A)^2 R^3/\beta$

ω_c measured natural frequency in cylinders, rad/sec

ω_A measured natural frequency in annular cylinders, rad/sec

APPARATUS AND PROCEDURE

Two zero gravity facilities at the Lewis Research Center were used to obtain the experimental data for this investigation. A complete description of these facilities, the experiment package, and the procedures for conducting the tests can be found in the appendixes. The test containers were flat bottomed annular cylinders. A typical annular cylinder is shown in figure 1. The annular cylinder consists of an outer cylinder of radius R, and an internal solid cylinder of radius r concentric with the outer cylinder.

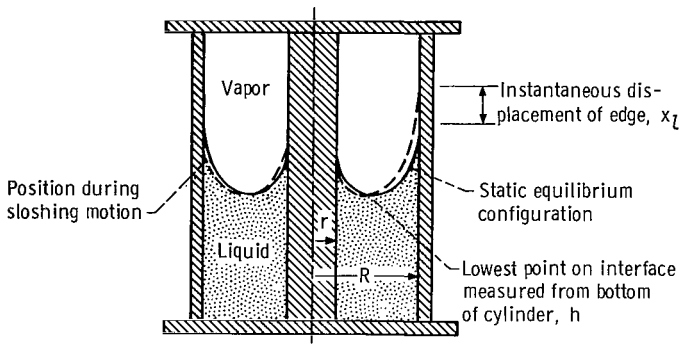

Figure 1. - Typical annular cylinder showing interface position during a slosh test.

TABLE I. - LIQUID PROPERTIES

[Properties at 20° C.]

Liquid	Surface tension, dynes/cm (or 10^{-5} N/cm)	Density, g/cm^3	Viscosity, cP (or 10^{-3} N-sec/m^2)
Freon-TF[a]	18.6	1.58	0.70
Anhydrous ethanol	22.3	.79	1.20
[b]FC-78	13.2	1.72	.82
Carbon tetrachloride	26.9	1.59	.97

[a]E. I. Dupont de Nemours and Co. registered trademark for a fluorocarbon solvent (trichlorotrifluoroethane).

[b]Minnesota Mining and Manufacturing Co. registered trademark for fluorocarbon solvent.

TABLE II. - SUMMARY OF TEST PARAMETERS

Liquid	Outer cylinder radius, R, cm	Annulus ratio, r/R	Measured natural frequency, ω_A, rad/sec	System acceleration, a, cm/sec^2	Bond number, Bo
Ethanol	0.70	0.09	17.1	0	0
Carbon tetrachloride	.70	.09	13.6	0	0
Ethanol	1.28	.10	6.7	0	0
Freon TF	1.28	.10	5.3	7.1	1.0
FC-78	1.28	.10	5.0	9.6	2.1
Freon TF	2.05	.10	4.1	14.0	5.0
Ethanol	.70	.09	55.6	980	16.9
Freon TF	1.28	.10	37.2	980	136
Ethanol	0.63	0.15	19.9	0	0
Freon TF	1.60	.16	32.5	980	211
Ethanol	1.33	0.20	6.7	0	0
Ethanol	1.33	.20	6.9	0	0
Carbon tetrachloride	1.33	.20	5.2	0	0
FC-78	1.33	.20	4.6	8.5	2.0
Freon TF	2.05	.20	3.8	13.9	5.0
Freon TF	1.33	.20	36.9	980	147
Ethanol	0.64	0.30	16.5	0	0
Ethanol	1.36	.30	5.7	0	0
Freon TF	1.36	.30	4.6	6.5	1.0
FC-78	1.36	.30	4.3	8.0	2.0
Freon TF	2.05	.30	3.8	13.9	5.0
Ethanol	.64	.30	52.3	980	14.4
Freon TF	1.36	.30	34.5	980	154
Ethanol	0.64	0.40	14.6	0	0
Ethanol	.64	.50	13.9	0	0
Carbon tetrachloride	.64	.50	10.1	0	0
Ethanol	1.30	.48	4.5	0	0
Freon TF	1.30	.48	4.1	7.0	1.0
FC-78	1.30	.48	4.0	9.1	2.0
Freon TF	2.05	.48	3.3	14.4	5.1
Ethanol	.64	.50	44.8	980	14.1
Freon TF	1.30	.48	32.3	980	140
Carbon tetrachloride	0.64	0.74	10.0	0	0
Ethanol	.64	.74	39.3	980	14.2
Freon TF	1.59	.73	26.2	980	210

The ratio of the radii of the inner cylinder and the outer cylinder r/R is defined as the annulus ratio. The outer cylinder radius R was varied from 0.63 to 2.05 centimeters. This resulted in annulus ratios varying from 0.09 to 0.74. The cylinders were fabricated from acrylic plastic.

The liquids used and their pertinent properties are listed in table I. All liquids had nearly zero degree static contact angles on the test container surfaces. For some of the liquids, a small quantity of dye was added to improve photographic quality. The dye had no measurable effect on the pertinent liquid properties. With the exception of the fluorocarbon solvents, the liquid properties were obtained from standard references. The fluorocarbon liquid properties were obtained from unpublished NASA data. The liquids were analytic reagent grade, except for the fluorocarbon solvents, which were precision cleaning grade.

The data were recorded photographically by a high speed camera. The slosh motion and displacement of the leading edge of the interface on the cylinder wall as a function of time was measured by using a film motion analyzer. The resulting periodic time-displacement curves were used to calculate the natural frequency for each test. A list of the test parameters and the measured data are presented in table II.

BACKGROUND INFORMATION

The Bond number ($Bo = aR^2/\beta$) is a nondimensional parameter indicating the relative magnitude of gravitational to capillary (surface tension) forces. The tests conducted in a near zero gravity environment yielded the zero Bond number data. Because some residual air drag was present for the near zero gravity tests, the Bond numbers were calculated using an acceleration value of 10^{-5} g. With this value of acceleration, the Bond numbers for the near zero gravity tests were on the order of 10^{-4} and are referred to as zero Bond numbers. The natural frequency of the liquid for the zero Bond number tests is determined solely by the restoring force due to surface tension. As the Bond number increases, the effect of the surface tension force on the natural frequency will diminish, and for high Bond numbers, the natural frequency of the liquid is dominated by the gravitational forces.

In reference 3, the governing equation for the natural frequency in right circular cylinders was correlated with known system parameters as a function of the Bond number and is given as follows:

$$\omega_c^2 = (2.6 + 1.84\ Bo)\frac{\beta}{R^3} \tag{1}$$

This equation is valid only for contact angles of very near zero degrees and for liquid depths greater than 2 cylinder radii. The constant 2.6 in equation (1) was experimentally obtained by the authors of reference 2 for zero Bond number conditions, and the value of 1.84 in equation (1) was obtained from the high Bond number result, which is found in many sources:

$$\omega_c^2 = 1.84 \frac{a}{R} \tag{2}$$

Equation (1) can be written in terms of the cylindrical natural frequency parameter, $\Omega_c^2 = \omega_c^2 R^3/\beta$ as follows:

$$\Omega_c^2 = (2.6 + 1.84\ \mathrm{Bo}) \tag{3}$$

From equation (3) when the Bo is approximately $1\frac{1}{2}$, the surface tension forces and the gravitational forces are equally important in determining the natural frequency. However, for a Bond number of 15, the surface tension forces are only about one-tenth as important as the gravitational forces in determining the natural frequency.

Theoretical investigations of the natural frequency in annular cylinders under high Bond number conditions (i.e., those Bond numbers where the surface tension effects are negligible) and deep liquid depths can be found in references 1, 4, and 5. The governing equation is as follows:

$$\omega_A^2 = f_1\left(\frac{r}{R}\right)\frac{a}{R} \tag{4}$$

where r/R is the annulus ratio. Theoretical values of $f_1(r/R)$ from reference 1 are listed in table III for discrete annulus ratios r/R.

TABLE III. - CALCULATED VALUES

OF $f_1(r/R)$ FROM REFERENCE 1

Annulus ratio, r/R	$f_1(r/R)$	Annulus ratio, r/R	$f_1(r/R)$
0.01	1.84080	0.5	1.35468
.1	1.80347	.6	1.26209
.2	1.70512	.7	1.18238
.3	1.58207	.8	1.11338
.4	1.46179	.9	1.05312

The general similarity between cylindrical and annular sloshing indicates that the natural frequency in annular cylinders should correlate in an analogous manner as in equation (3). An annular natural frequency parameter is assumed to be dependent on both a gravitational term and a capillary term with coefficients that are functions of the annulus ratio r/R. The following empirical relation was proposed to be valid:

$$\Omega_A^2 = f_2\left(\frac{r}{R}\right) + f_1\left(\frac{r}{R}\right)Bo \tag{5}$$

where $\Omega_A^2 = \omega_A^2 R^3/\beta$ is the annular natural frequency parameter. The value of the function $f_2(r/R)$ was determined from the experimental tests of this study conducted in a zero Bond number environment, and $f_1(r/R)$ is from high Bond number results (ref. 1) given in table III. The values of $f_1(r/R)$ and $f_2(r/R)$ will determine the relative importance of the gravitational forces and the surface tension forces on determining the natural frequency in annular cylinders.

RESULTS AND DISCUSSION

Interface Behavior During a Typical Slosh Mode

The liquid-vapor interface shape is shown schematically in figure 1 for both the static equilibrium configuration prior to a slosh mode and the interface shape during a sloshing motion. The lowest point on the interface h, measured from the cylinder bottom, was always kept greater than 2 cylinder radii to eliminate effects of the cylinder bottom on the natural frequency. The instantaneous displacement of the interface edge at the outer cylinder wall X_l was used to describe the motion of the liquid. In all cases the maximum initial value of X_l was less than 0.25 R. For these small amplitudes, the motion of the interface edge was a damped harmonic with no measurable decrease in frequency.

A series of photographs describing the interface behavior during a typical test is presented in figure 2. The liquid-vapor interface, initially at rest in figure 2(a) was allowed to form its equilibrium interface shape corresponding to the test Bond number (fig. 2(b)). The slosh motion was produced by accelerating the experiment tank laterally (fig. 2(c)) and then imparting a quick stop impulse (fig. 2(d)). Although the interface distorted as a result of the impulse, it quickly assumed a normal sloshing motion as can be seen in the subsequent photographs of figures 2(e) to (h). A typical time history of the motion of the interface is shown in figure 3. These time-displacement curves were used to calculate the natural frequency for each test.

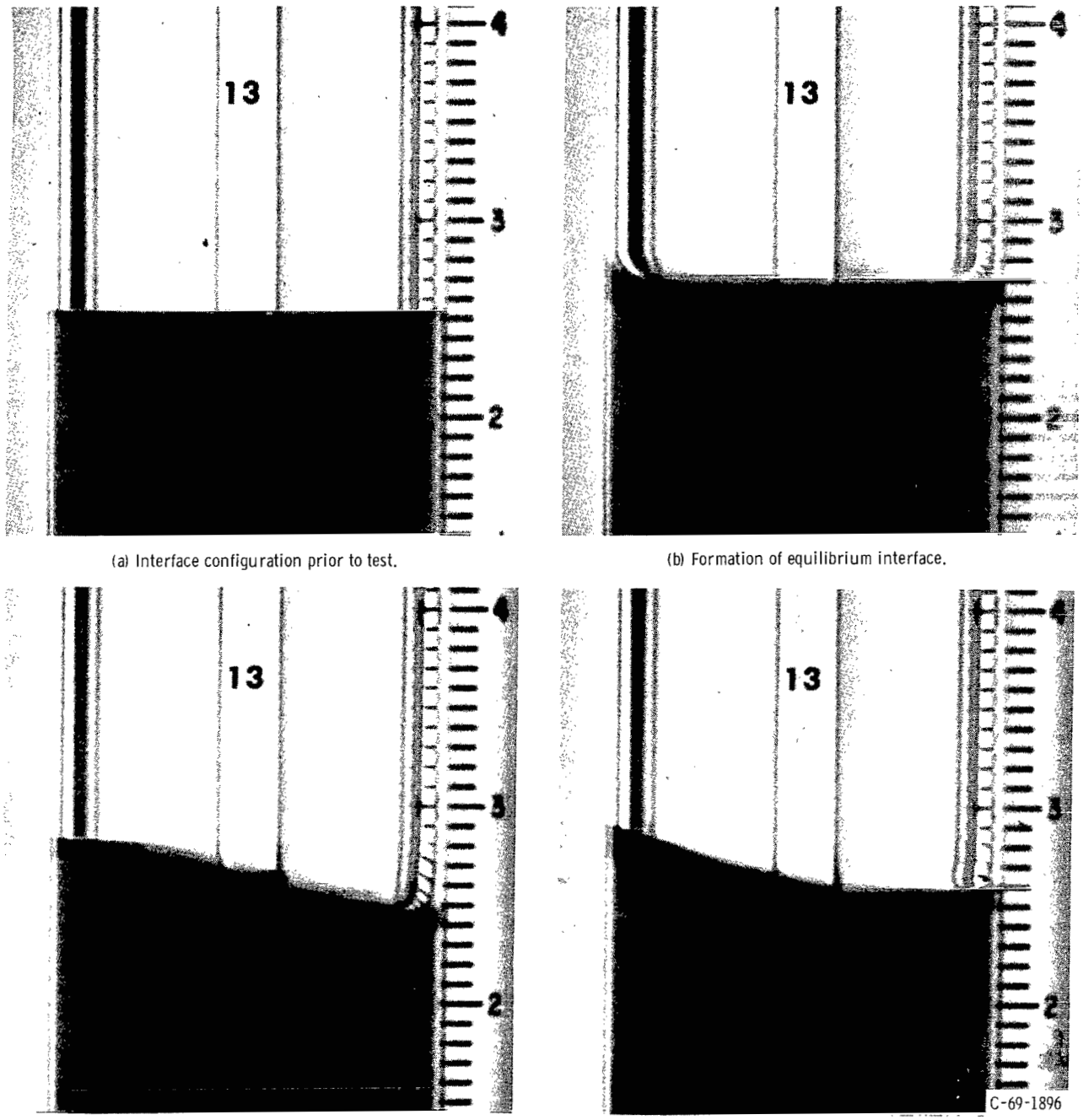

(a) Interface configuration prior to test.

(b) Formation of equilibrium interface.

(c) Lateral disturbance initiates sloshing motion.

(d) Impulse at end of stroke.

Figure 2. - Typical slosh motion of the liquid-vapor interface. Test Bond number, 5.0; system acceleration, 13.9 centimeters per second squared; outer cylinder radius, 2.05 centimeters; annulus ratio, 0.2; test liquid, Freon-TF.

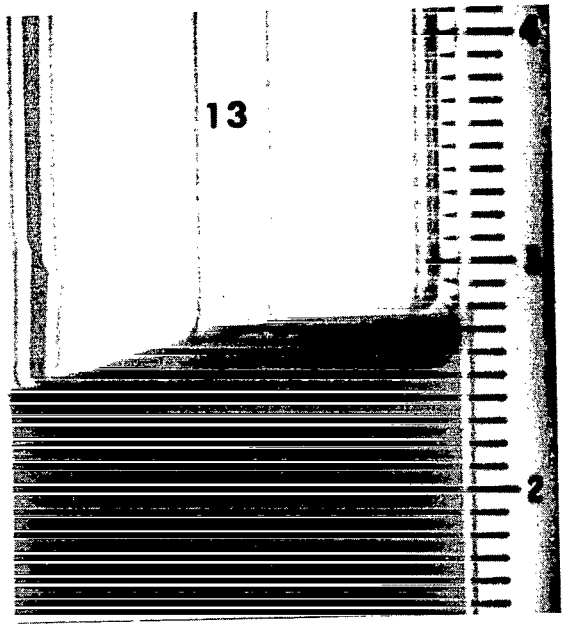

(e) Behavior of interface immediately after impulse.

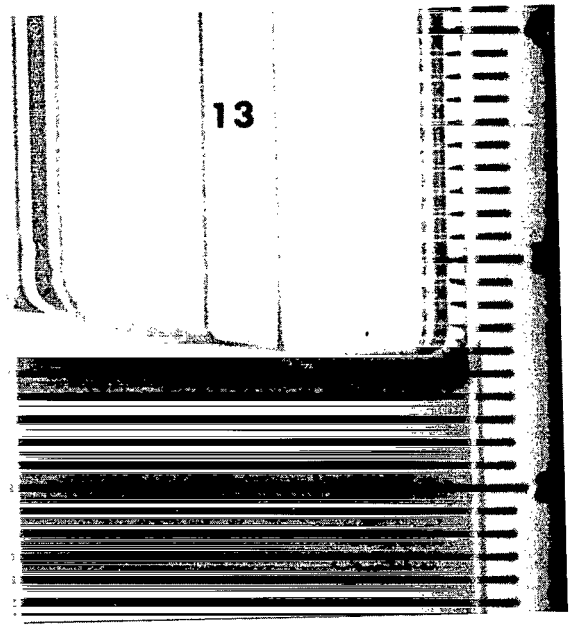

(f) Sloshing motion obtained.

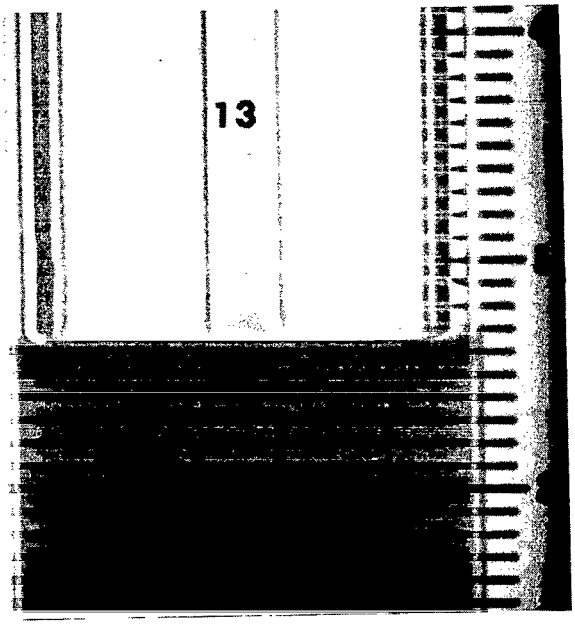

(g) Pass through equilibrium.

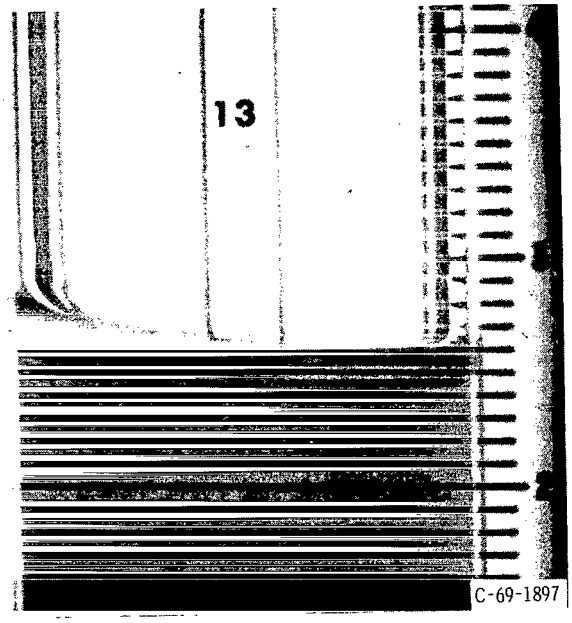

(h) Decaying interface oscillations.

Figure 2. - Concluded.

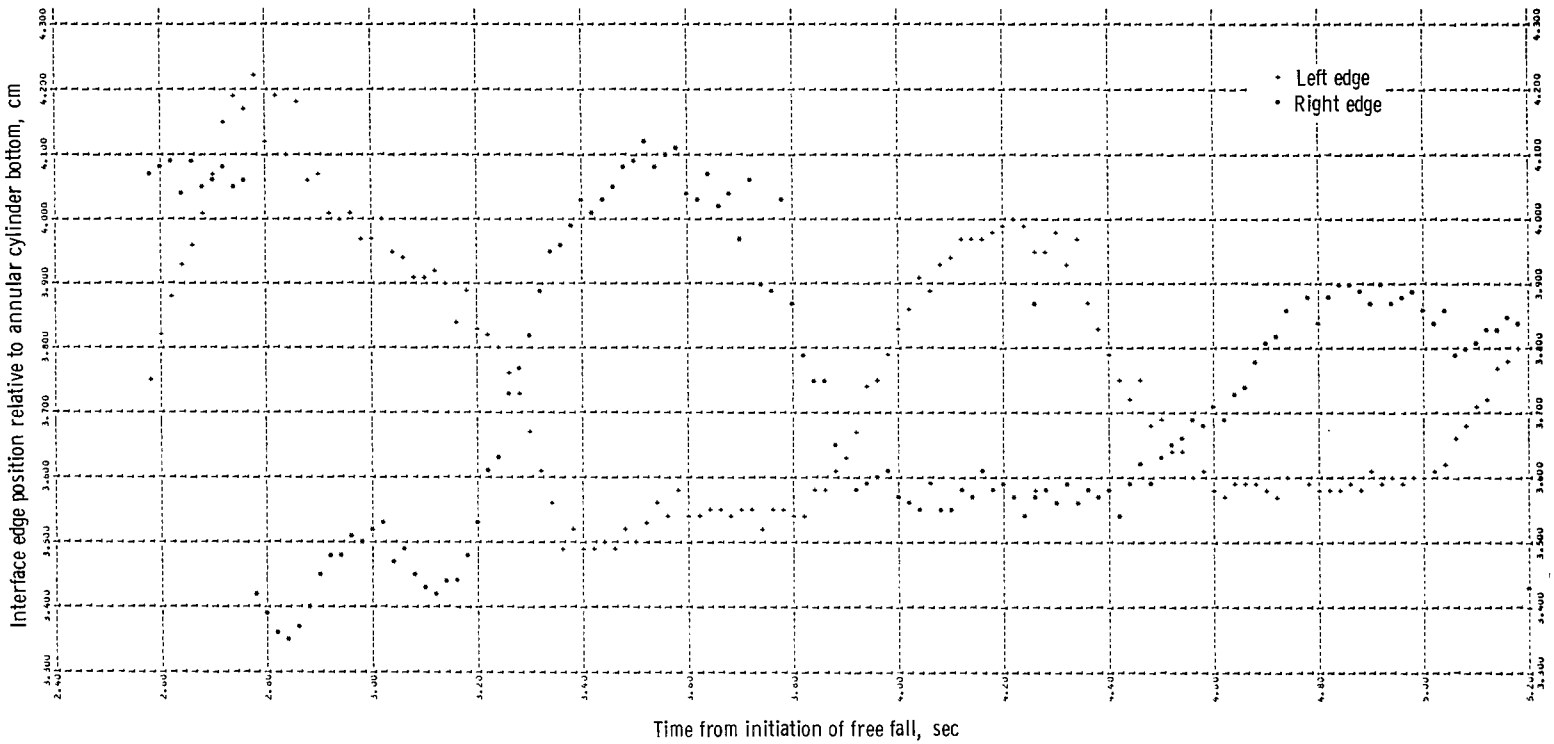

Figure 3. - A typical time history of lateral sloshing in annular cylinders. Test Bond number, 2.0; system acceleration, 9.6 centimeters per second squared; outer cylinder radius, 1.28 centimeters; annulus ratio, 0.1; test liquid, FC-78.

Zero Bond Number Natural Frequency

Earlier, it was proposed that the natural frequency in annular cylinders may be correlated by using the annular natural frequency parameter

$$\Omega_A^2 = \frac{\omega_A^2 R^3}{\beta}$$

The results of the zero Bond number study are presented in figure 4 where the square root of the annular natural frequency parameter is plotted against the annulus ratio. Figure 4 shows that the natural frequency in annular cylinders does correlate in a similar manner to that in cylinders and that the annular natural frequency parameter Ω_A^2 depends only on the annulus ratio r/R under zero Bond number conditions.

The annular natural frequency parameter Ω_A^2 increases with the addition of an annulus, reaches a maximum at an annulus ratio of 0.2, and then decreases. The point on the curve at (r/R) = 0, a simple cylinder, was obtained from reference 2. For $0 < (r/R) \leq 0.30$, the annular natural frequency parameter is greater than the cylindrical natural frequency parameter (r/R) = 0, but for annulus ratios greater than 0.40, it is lower. Because at zero Bond number the natural frequency is determined by the capillary forces, the shape of the curve of figure 4 is an indication of the variation of capillary forces with annulus ratio. A similar indication of the variation of capillary forces with this geometry is found in the theroetical annular stability work of reference 6 where the variation of critical Bond number with annulus ratio was studied.

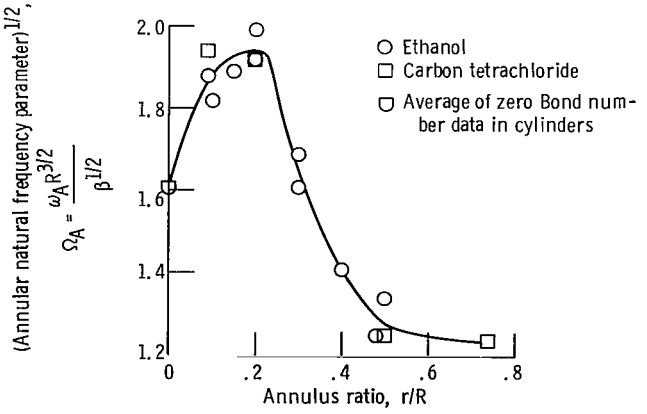

Figure 4. - Natural frequency in annular cylinders under zero Bond number conditions.

TABLE IV. - ZERO BOND NUMBER

EMPIRICAL CONSTANTS AS

FUNCTION OF ANNULUS RATIO

Annulus ratio, r/R	$f_2(r/R)$	Annulus ratio, r/R	$f_2(r/R)$
0	2.6	0.4	2.0
.1	3.6	.5	1.6
.2	3.8	.6	1.6
.3	2.7	.7	1.5

Values of Ω_A can be determined from figure 4. From the proposed general relation for the annular natural frequency (eq. (5)), the values of Ω_A are $\sqrt{f_2(r/R)}$ because the Bo = 0. Selected values of $f_2(r/R)$ are listed in table IV. Accuracy of these values is within ± 0.1.

Effect of Bond Number on the Natural Frequency

We refer to the proposed empirical equation for the annular natural frequency (eq. (5)):

$$\Omega_A^2 = f_2\left(\frac{r}{R}\right) + f_1\left(\frac{r}{R}\right) Bo$$

where $f_2(r/R)$ is the constant obtained from the zero Bond number data (table IV) and $f_1(r/R)$ is determined from high Bond number data (table III). Using these constants, lines were drawn in figure 5 for annulus ratios of 0.1, 0.2, 0.3, and 0.5 according to equation (5). The data for all Bond numbers from this study are shown in the figure and indicate excellent agreement with the empirical equation.

The measured natural frequency data in annular cylinders for all Bond numbers can be normalized with respect to the natural frequency in cylinders and are shown in figure 6 as a function of the annulus ratio r/R. The solid line is the zero Bond number

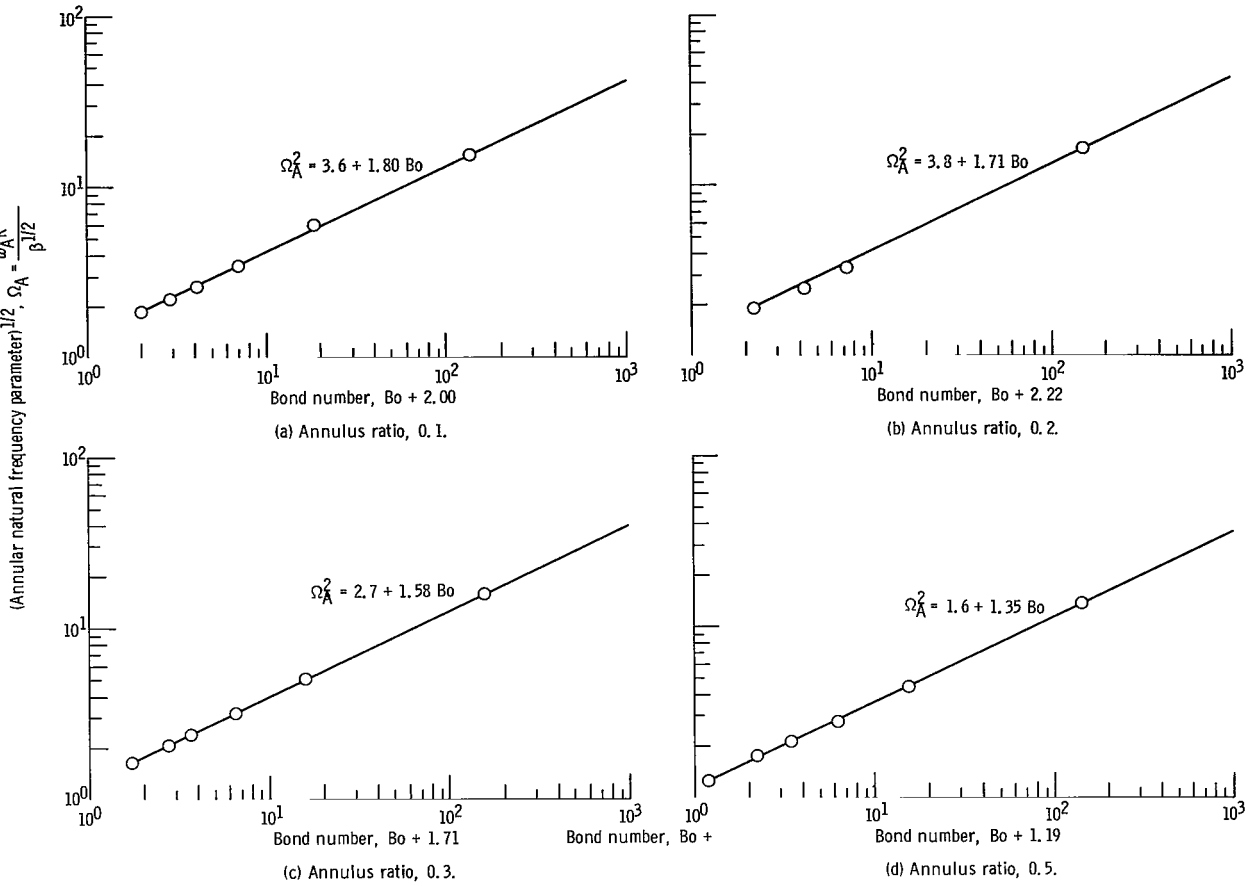

Figure 5. - Correlation of natural frequency with the Bond number.

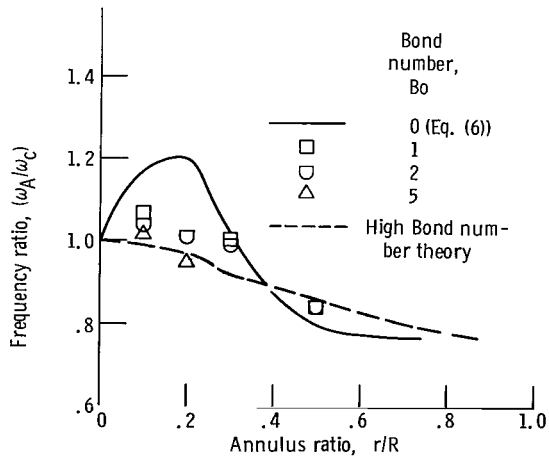

Figure 6. - Natural frequency envelope for annular cylinders under all Bond numbers.

data of figure 4 and is obtained by a substitution of the values of f_2 from table IV into the following equation:

$$\left.\frac{\omega_A}{\omega_c}\right|_{Bo=0} = \left[\frac{f_2\left(\frac{r}{R}\right)}{2.6}\right]^{1/2} \tag{6}$$

The value 2.6 in equation (6) is $f_2(r/R)$ at $r = 0$. The dashed line represents the high bond number results of reference 1 and is obtained by a substitution of the values of f_1 from table III into the following equation:

$$\left.\frac{\omega_A}{\omega_c}\right|_{Bo\to\infty} = \left[\frac{f_1\left(\frac{r}{R}\right)}{1.84}\right]^{1/2} \tag{7}$$

The value 1.84 in equation (7) is $f_1(r/R)$ at $r = 0$.

The data at Bond numbers of 1, 2, and 5 for the frequency ratios were obtained by measuring ω_A from the experimental data from this study and dividing the result by ω_c from equation (1). The frequency ratio for all Bond numbers and all annulus ratios lie in the two envelopes formed by the intersecting curves (eqs. (6) and (7)). If the natural frequency in annular cylinders is desired at other annulus ratios, the constants $f_1(r/R)$ and $f_2(r/R)$ can be chosen from figure 6 and inserted into equation (5). The natural frequency at any Bond number can then be predicted.

SUMMARY OF RESULTS

An experimental investigation was conducted to determine the natural frequency of liquids in annular cylinders. The study was conducted over a range of Bond numbers from zero to approximately 200 using liquids that exhibited near zero degree contact angles on the acrylic walls of the annular cylinders. The radius of the outer cylinder was varied from 0.63 to 2.05 centimeters, and the annulus ratios were varied between 0.09 and 0.74. The liquid-vapor interface was greater than 2 outer cylinder radii from the tank bottom. This study, which was restricted to small amplitude motion yielded the following results:

h

1. The annular natural frequency parameter Ω_A^2 depends on the annulus ratio r/R under zero Bond number conditions. For annulus ratios up to and including 0.3, Ω_A^2 was higher than the corresponding zero Bond number case with a simple cylinder. For annulus ratios greater than or equal to 0.4, Ω_A^2 was lower than the corresponding zero Bond number case with a simple cylinder. At an annulus ratio of approximately 0.2, Ω_A^2 reached a maximum.

2. The natural frequency at all Bond numbers ($Bo = aR^2/\beta$) was dependent on the annulus ratio r/R. The relation between the natural frequency, annulus ratio, and the Bond number was described by the following empirical equation: $\Omega_A^2 = f_2(r/R) + f_1(r/R)Bo$. The function f_2 was empirically determined from zero Bond number data; and the function f_1 was available from theoretical high Bond number data. The annular natural frequency parameter was in good agreement with the empirical relation for all Bond numbers at annulus ratios of 0.1, 0.2, 0.3, and 0.5.

Lewis Research Center,
National Aeronautics and Space Administration,
Cleveland, Ohio, June 13, 1969,
124-09-17-01-22.

APPENDIX A

APPARATUS AND PROCEDURE FOR 2.2-SECOND FACILITY

Test Facility

The Lewis Research Center 2.2-Second Zero-Gravity Facility (fig. 7) consists of a building 6.4 meters (21 ft) square by 30.5 meters (100 ft) tall. Contained within this building is a drop area 27 meters (89 ft) long with a cross section 1.5 by 2.75 meters (5 by 9 ft).

The service building has, as its major elements, a shop and service area, calibration room, and controlled environment room. Those components of the experiment that require special handling are prepared in the facility controlled environment room (fig. 8). This air-conditioned room, supplied with filtered air, contains an ultrasonic cleaning system and the laboratory equipment necessary for handling test liquids.

Mode of operation. - A 2.2-second period of free fall is obtained by allowing the experiment package to free fall from the top of the drop area. To minimize drag on the experiment package, it is enclosed in a drag shield, designed with a high ratio of weight to frontal area and a low drag coefficient. The relative motion of the experiment package with respect to the drag shield during a test is shown in figure 9. Throughout the test, the experiment package and drag shield fall freely and independently of each other; that is, no guide wires, electrical lines, etc., are connected to either. Therefore, the only force acting on the freely falling experiment package is the air drag associated with the relative motion of the package within the drag shield. This air drag results in an equivalent gravitational acceleration acting on the experiment, which is estimated to be below 10^{-5} g's.

Release system. - The experiment package, installed within the drag shield, is suspended at the top of the drop area by means of a highly stressed music wire attached to the release system. This release system consists of a double-acting air piston with a hard-steel knife edge attached to the piston. Pressurization of the air cylinder drives the knife edge against the wire, which is backed by an anvil. The resulting notch causes the wire to fail, smoothly releasing the experiment. No measurable disturbances are imparted to the package by this release procedure.

Recovery system. - After the experiment package and drag shield have traversed the total length of the drop area, they are recovered by decelerating in a 2.2-meter (7-ft) deep container filled with sand. The deceleration rate (averaging 15 g's) is controlled by selectively varying the tips of the deceleration spikes mounted on the bottom of the drag shield (fig. 7). At the time of impact of the drag shield in the decelerator container, the experiment package has traversed the vertical distance within the drag shield (compare figs. 9(a) and (c)).

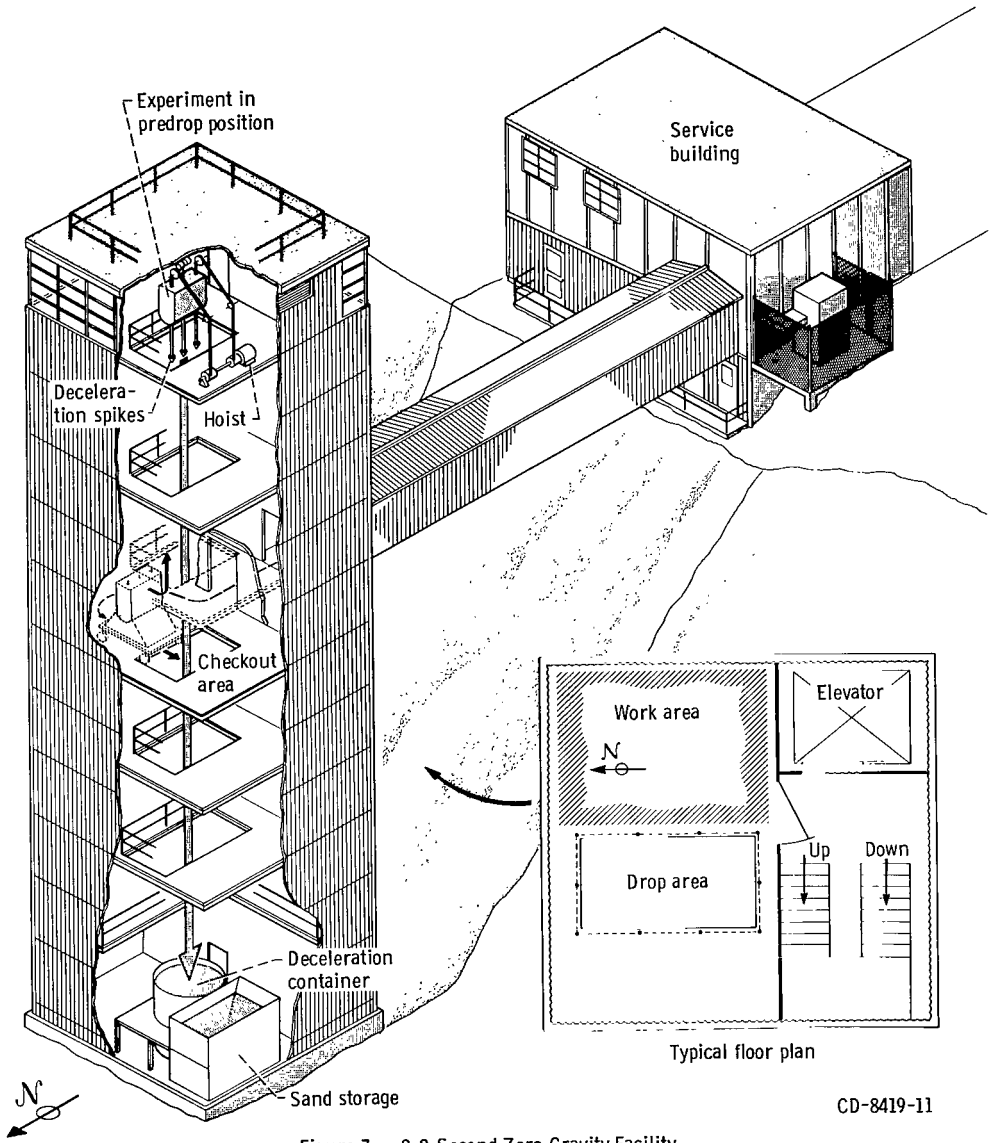

Figure 7. - 2.2-Second Zero Gravity Facility.

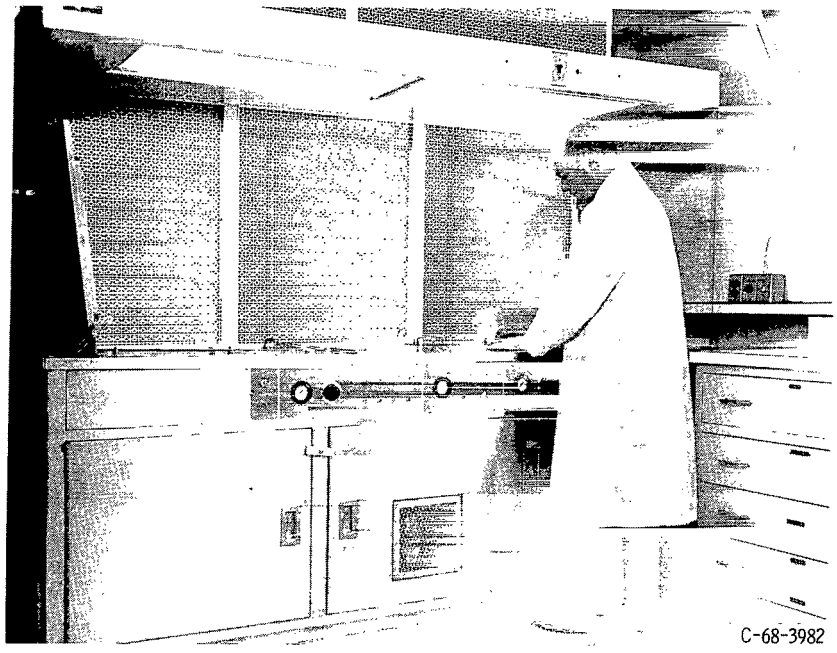

C-68-3982

(a) Ultrasonic cleaning system.

C-68-3983

(b) Laboratory equipment.

Figure 8. - Controlled environment room.

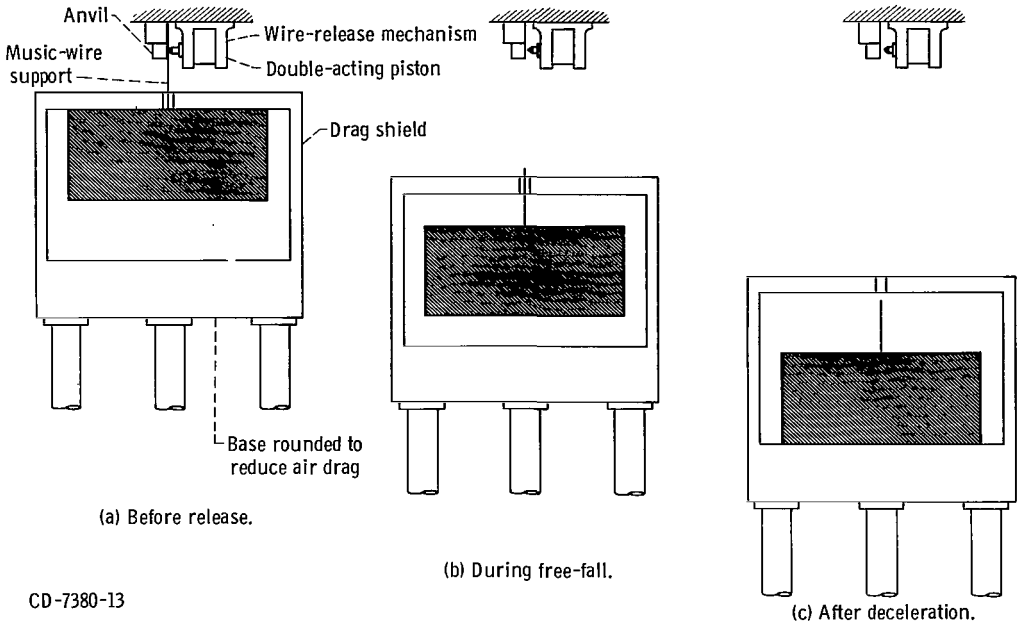

Figure 9. - Position of experiment package and drag shield before, during, and after test drop.

Experiment Package

The experiment package used to obtain the data in this facility consisted of an aluminum frame in which were mounted the test container, air cylinder and slide, a 16-millimeter high-speed motion picture camera, a backlighting scheme, and auxiliary equipment. A schematic drawing of the apparatus is shown in figure 10. The auxiliary equipment included batteries, a sequence timer, and a digital clock. The air cylinder was used to apply a lateral disturbance to the low friction slide. The test containers (described previously) were rigidly mounted on the low friction slide.

Test Procedure

Experiment preparation. - The annular cylinders were prepared in the controlled environment room (fig. 8). Contamination of the liquid and cylinder, which would alter the surface tension and contact angle, was carefully avoided. The test cylinders were cleaned ultrasonically in a detergent-water solution, rinsed with a distilled-water - methanol solution, and dried in a warm air dryer. The test cylinders were rinsed with the test liquid, filled to the desired liquid depth and sealed to prevent contamination. They were then mounted on the low friction slide. During the test, a predetermined time increment was allowed so that the interface could approach its equilibrium shape. The

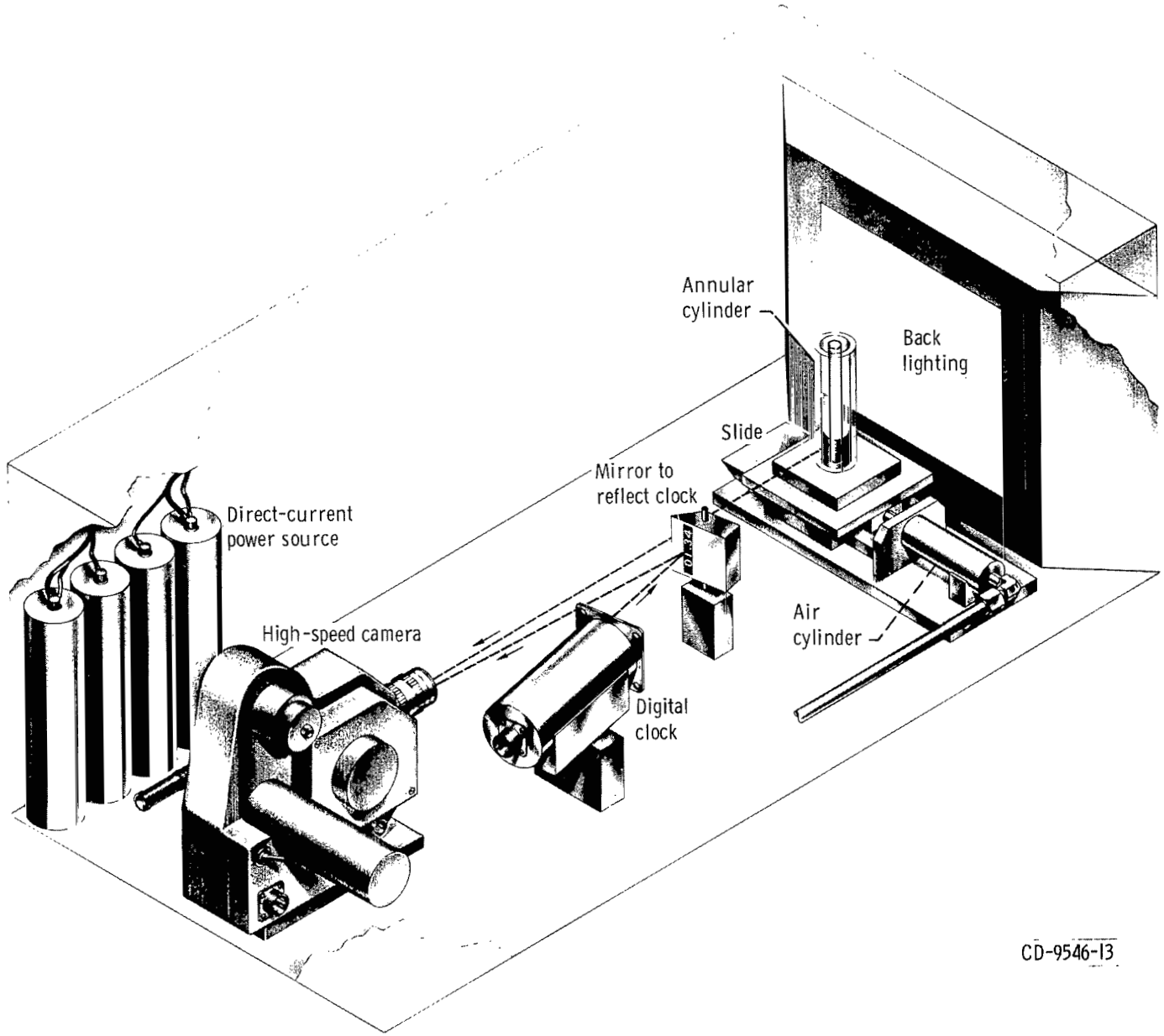

Figure 10. - Experimental apparatus.

lateral impulse was applied, displacing the interface from its equilibrium position. The subsequent oscillations of the interface edge were recorded on film.

Procedure for test drop. - Electrical timers were used to control the initiation and duration of all functions programmed during the drop. The experiment package is balanced and then positioned with the prebalanced drag shield. The wire support is attached to the experiment package through an access hole in the shield (see fig. 9(a)). Properly sized tips are installed on the drag shield. Then the drag shield, with the experiment package inside, is hoisted to the predrop position at the top of the facility (fig. 7) and connected to an external electrical power source. The wire support is attached to the release system, and the entire assembly is suspended from the wire. After final electrical checks and switching to internal power, the system is released. After completion of the test, the experiment package and drag shield are returned to the preparation area.

APPENDIX B

APPARATUS AND PROCEDURE FOR 5- TO 10-SECOND FACILITY

Test Facility

The Lewis Research Center's 5- to 10-Second Zero-Gravity Facility is shown in figure 11. This facility consists of a concrete-lined, 8.5-meter (28-ft) diameter shaft that extends 155 meters (510 ft) below ground level. A steel vacuum chamber, 6.1 meters (20 ft) in diameter and 143 meters (470 ft) high, is contained within the concrete shaft. The pressure in this vacuum chamber is reduced to 13.3 newtons per square meter (1.3×10^{-4} atm) by utilizing the wind tunnel exhaust system and an exhaust system located in the facility.

The ground-level service building has, as its major elements, a shop area, a control room, and a clean room. Assembly, servicing, and balancing of the experiment vehicle are accomplished in the shop area. Tests are conducted from the control room, which contains the exhauster control system, the experiment vehicle predrop checkout and control system, and the data retrieval system. Those components of the experiment that are in contact with the test liquid are prepared in the facility's class 10 000 clean room. The major elements of the clean room are an ultrasonic cleaning system (fig. 12) and a class 100 laminar-flow work station for preparing those experiments requiring more than normal cleanliness.

Mode of operation. - The Zero-Gravity Facility has two modes of operation. One is to allow the experiment vehicle to free fall from the top of the vacuum chamber, which results in nominally 5 seconds of free fall time. The second mode is to project the experiment vehicle upwards from the bottom of the vacuum chamber by a high-pressure pneumatic accelerator located on the vertical axis of the chamber. The total up and down trajectory of the experiment vehicle results in nominally 10 seconds of free fall time. The 5-second mode of operation was used for this experimental study.

In either mode of operation, the experiment vehicle falls freely; that is, no guide wires, electrical lines, etc., are connected to the vehicle. Therefore, the only force acting on the freely falling experiment vehicle is due to residual-air drag. This results in an equivalent gravitational acceleration acting on the experiment, which is estimated to be of the order of 10^{-5} g maximum.

Recovery system. - After the experiment vehicle has traversed the total length of the vacuum chamber, it is decelerated in a 3.6-meter (12-ft) diameter, 6.1-meter (20-ft) deep container which is located on the vertical axis of the chamber and filled with small pellets of expanded polystyrene. The deceleration rate (averaging 32 g) is controlled by the flow of pellets through the area between the experiment vehicle and the wall of the

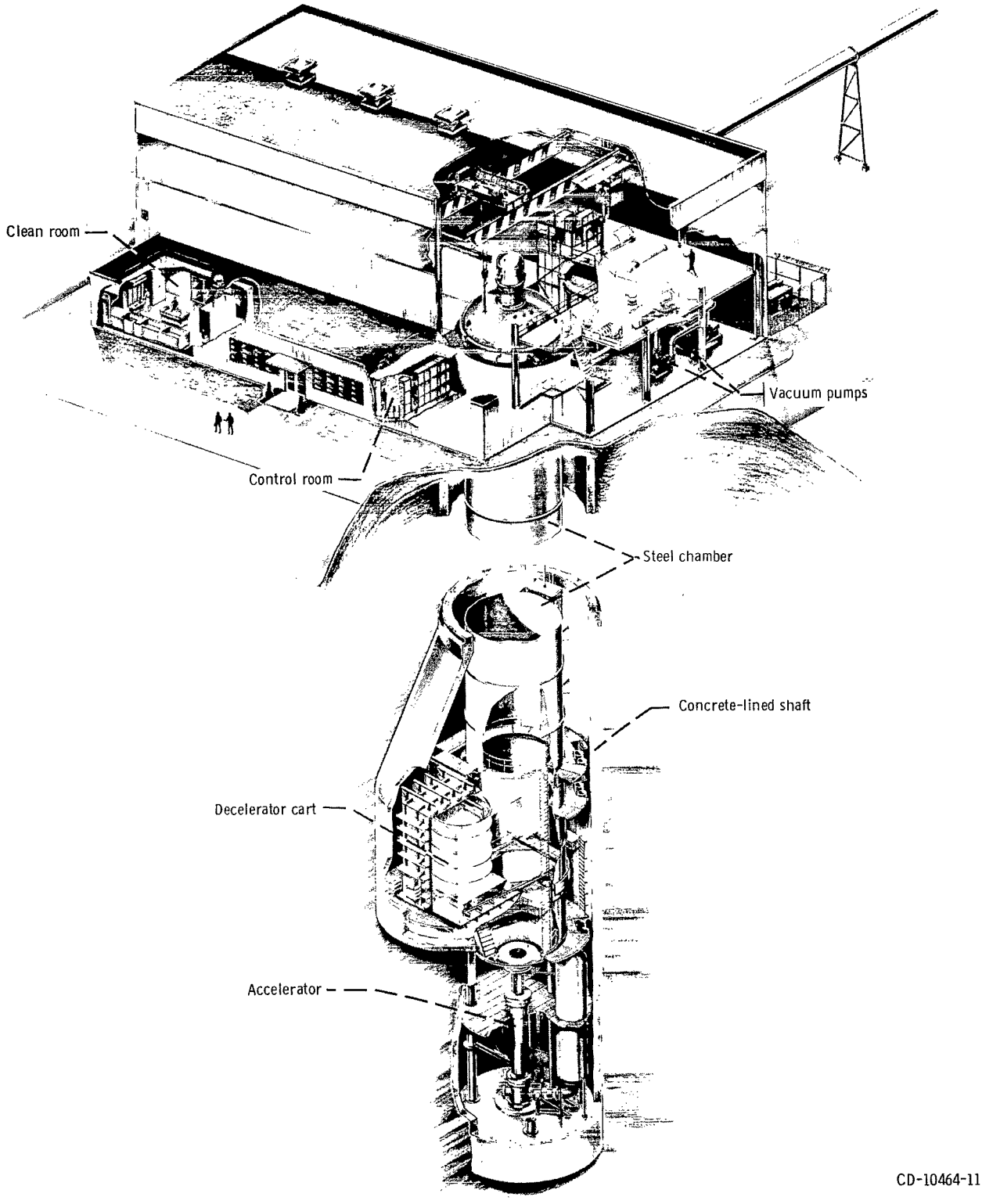

Figure 11. - Schematic diagram of 5- to 10-Second Zero-Gravity Facility.

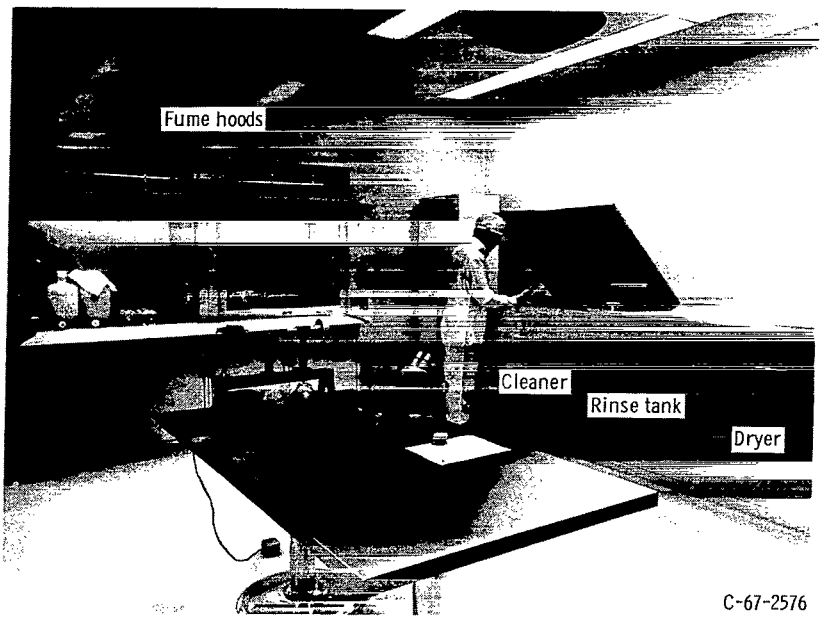

Figure 12. - Clean room.

deceleration container. This deceleration container is mounted on a cart that is retracted prior to utilizing the 10-second mode of operation. In this mode of operation, the cart is deployed after the experiment vehicle is projected upwards by the pneumatic accelerator.

Experiment Vehicle

The experiment vehicle used to obtain the data for this experimental study is shown in figure 13. The overall vehicle height (exclusive of the support shaft) is 2.7 meters (8.9 ft) and the largest diameter is 1.06 meters (3.5 ft). The vehicle consists of three basic sections: A thrust system section, which is contained in the conical base, an experiment section, which is housed in the cylindrical midsection, and a telemetry section, which is contained in the top fairing.

Thrust system. - The conical base of the experiment vehicle contains the cold-gas thrust system, is capable of producing thrusts ranging from 13 to 130 newtons (3 to 30 lb) for time durations in excess of 5 seconds. Prior to installation on the experiment vehicle, the thrust system was calibrated on a static thrust calibration stand located in the facility vacuum chamber. The calibration was conducted at pressure levels corresponding to test-drop conditions. A null-balance, load-cell system was used to record the thrust time history as a function of thrust nozzle inlet pressure and nozzle-size.

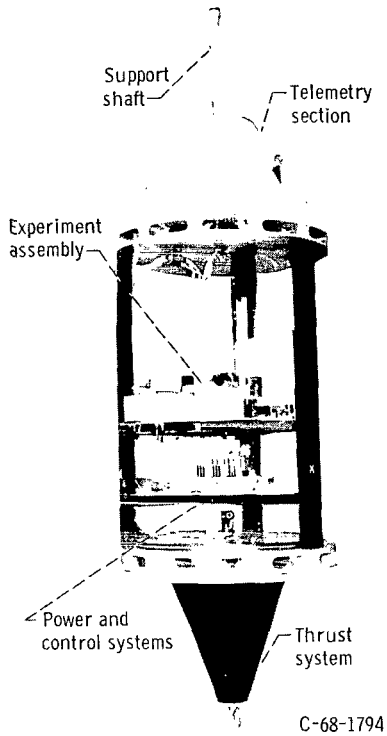

Figure 13. - Experiment vehicle.

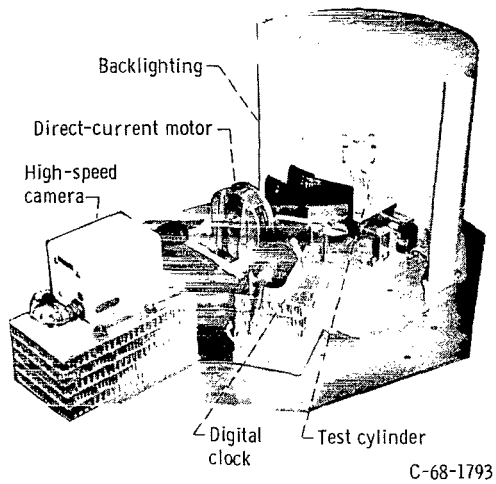

Figure 14. - Experiment assembly tray.

Telemetry system. - The on-board telemetry system is an FM/FM system with 18 continuous channels. During a test drop, telemetry is used to continuously record thrust nozzle inlet pressure, two low-g accelerometers, and other parameters pertinent to the experiment.

Experiment. - The experiment section consisted of the test container tray plus electrical power and control system equipment mounted in the cylindrical section of the experiment vehicle. This section was 1.7 meters long. The test container tray (fig. 14), included the test container, slosh mechanism, camera, and lighting and timing systems. The test container, mounted on a slide carriage, was connected to a direct-current motor. The motor supplied a single, lateral pulse to the carriage and container. The ensuing slosh motion was recorded by a high speed motion picture camera. Elapsed time was obtained from a digital clock.

Test Procedure

Cleaning, filling, and hermetic sealing of the annular cylinders was conducted in the facility's clean room (fig. 12) using the same procedure as that described in appen-

dix A. The annular cylinders were then installed in the experiment vehicle. During the test, a predetermined time increment was allowed so that the interface could approach its equilibrium shape. The lateral impulse was supplied, displacing the interface from its equilibrium position. The subsequent oscillations of the interface edge were recorded on film.

Electrical timers on the experiment vehicle control the initiation and duration of all functions programmed during the drop. The experiment vehicle is then balanced about its vertical axis to insure an accurate drop trajectory and thrust alinement with respect to the experiment tank. Accurate thrust alinement is necessary to provide an axisymmetric, equilibrium liquid-vapor interface shape.

The vehicle is then positioned at the top of the vacuum chamber as shown in figure 15. It is suspended by the support shaft on a hinged-plate release mechanism. During vacuum chamber pumpdown and prior to release, monitoring of experiment vehicle systems is accomplished through an umbilical cable attached to the top of the support shaft. Electrical power is supplied from ground equipment. The system was then switched to internal power a few minutes before release. The umbilical cable is remotely pulled from the support shaft 0.5 second prior to release. The thrust system is

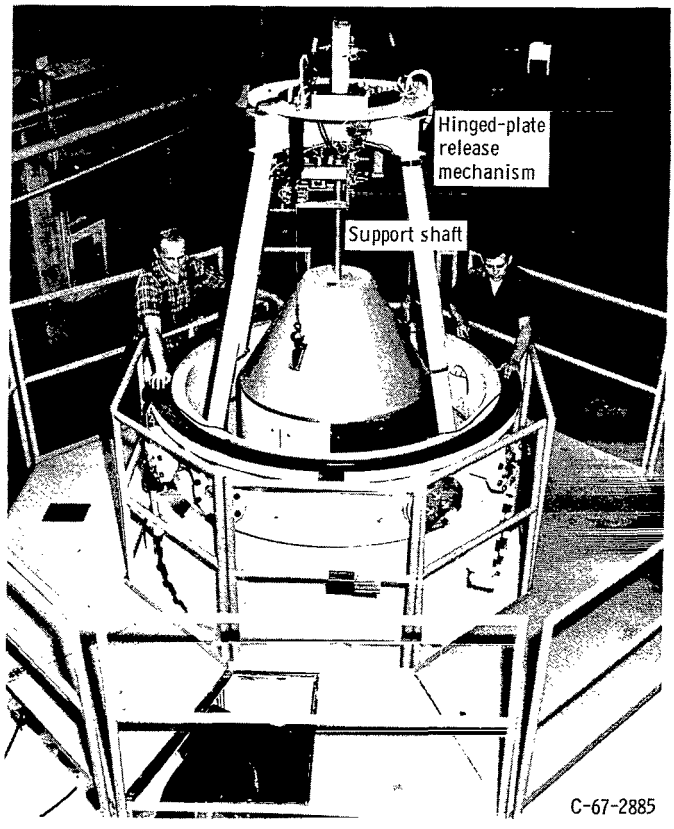

Figure 15. - Vehicle position prior to release.

activated 0.2 second before release to allow the thrust to reach steady-state conditions. The vehicle is released by pneumatically shearing a bolt that was holding the hinged-plate in the closed position. No measurable disturbances are imparted to the experiment vehicle by this release procedure.

The total free-fall test time obtained in this mode of operation is 5.16 seconds. Approximately 0.13 second before the experiment vehicle enters the deceleration container, the thrust system is shut down to avoid dispersing the deceleration material. During the test drop, the vehicle's trajectory and deceleration are monitored on closed-circuit television. Following the test drop, the vacuum chamber is vented to the atmosphere and the experiment vehicle is returned to ground level.

REFERENCES

1. Abramson, H. Norman; and Silverman, S.: Lateral Sloshing in Moving Containers. The Dynamic Behavior of Liquids in Moving Containers, with Applications to Space Vehicle Technology. NASA SP-106, 1966, pp. 13-78.

2. Salzman, Jack A.; Labus, Thomas L.; and Masica, William J.: An Experimental Investigation of the Frequency and Viscous Damping of Liquids During Weightlessness. NASA TN D-4132, 1967.

3. Salzman, Jack A.; and Masica, William J.: Lateral Sloshing in Cylinders Under Low-Gravity Conditions. NASA TN D-5058, 1969.

4. Bauer, Helmut F.: Theory of the Fluid Oscillations in a Circular Cylindrical Ring Tank Partially Filled with Liquid. NASA TN D-557, 1960.

5. Okhotsimskii, D. E.: Theory of the Motion of a Body with Cavities Partly Filled with Liquid. NASA TT F-33, 1960.

6. Seebold, J. G.; Hollister, M. P.; and Satterlee, H. M.: Capillary Hydrostatics in Annular Tanks. J. Spacecraft Rockets, vol. 4, no. 1, Jan. 1967, pp. 101-105.

NASA-Langley, 1969 —— 12 E-5103

NATIONAL AERONAUTICS AND SPACE ADMINISTRATION
WASHINGTON, D. C. 20546
OFFICIAL BUSINESS

FIRST CLASS MAIL

POSTAGE AND FEES PAID
NATIONAL AERONAUTICS AND
SPACE ADMINISTRATION

"The aeronautical and space activities of the United States shall be conducted so as to contribute . . . to the expansion of human knowledge of phenomena in the atmosphere and space. The Administration shall provide for the widest practicable and appropriate dissemination of information concerning its activities and the results thereof."

—NATIONAL AERONAUTICS AND SPACE ACT OF 1958

NASA SCIENTIFIC AND TECHNICAL PUBLICATIONS

TECHNICAL REPORTS: Scientific and technical information considered important, complete, and a lasting contribution to existing knowledge.

TECHNICAL NOTES: Information less broad in scope but nevertheless of importance as a contribution to existing knowledge.

TECHNICAL MEMORANDUMS: Information receiving limited distribution because of preliminary data, security classification, or other reasons.

CONTRACTOR REPORTS: Scientific and technical information generated under a NASA contract or grant and considered an important contribution to existing knowledge.

TECHNICAL TRANSLATIONS: Information published in a foreign language considered to merit NASA distribution in English.

SPECIAL PUBLICATIONS: Information derived from or of value to NASA activities. Publications include conference proceedings, monographs, data compilations, handbooks, sourcebooks, and special bibliographies.

TECHNOLOGY UTILIZATION PUBLICATIONS: Information on technology used by NASA that may be of particular interest in commercial and other non-aerospace applications. Publications include Tech Briefs, Technology Utilization Reports and Notes, and Technology Surveys.

Details on the availability of these publications may be obtained from:

SCIENTIFIC AND TECHNICAL INFORMATION DIVISION

NATIONAL AERONAUTICS AND SPACE ADMINISTRATION

Washington, D.C. 20546